Front. Electr. Electron. Eng. China (2006) 3: 345–349
DOI 10.1007/s11460-006-0029-9

RESEARCH ARTICLE

LIU Shao-dong, JIAO Yong-chang, ZHANG Fu-shun

Effect of random surface errors on radiation characteristics of the side-fed offset Cassegrain antenna

Abstract In this paper the average power pattern of the side-fed offset Cassegrain (SFOC) dual reflector antenna is analyzed, and the effect of the random surface error on radiation characteristics of the antenna is introduced. Here, the random surface error is defined as the error of the standard reflector in its normal direction and the errors in a small zone of the reflector are considered as equal. We also assume that the phase error on the aperture led by the random surface error obeys a Gaussian distribution with zero mean, under which the expression of the average power pattern is deduced. Finally, the data related to the radiation characteristics of the antenna are calculated and the corresponding curves are presented. The obtained results can be used for the user to determine the manufacturing accuracy of the reflector of the SFOC antennas.

Keywords reflector antenna, average power pattern, random surface error, Gaussian distribution

1 Introduction

Reflector antennas usually work at the higher frequency band, and its radiation characteristics are greatly affected by various errors [1, 2]. These errors mainly include the random installation error and the random surface error. The latter is due to the technology level for manufacturing and testing the reflectors [3–5], which is an error source that should be considered in the production of the reflector antennas. High accuracy requirement may guarantee the performance of the reflector antennas, but it will raise the manufacturing costs. Sometimes the accuracy requirement is unrealistic, since it is restricted by the technology level and the practical working environment. Therefore, in the design of the reflector antennas, the effect of various errors on the antennas performance must be analyzed, and the reasonable tolerance requirements according to the desired performance should be provided. In this paper, the average power pattern of the SFOC reflector antenna is calculated. The effects of the random surface error on the antenna's gain and side lobe level are also analyzed by the numerical method, and some simulation data as well as curves are presented, which will be helpful for determining the reasonable tolerance requirements for manufacturing the reflector antenna.

2 Geometry of the SFOC antenna

The geometry of the SFOC antenna [6] is shown in Fig. 1, in which the main reflector is the paraboloid (focal length f), and the subreflector is the hyperboloid (interfocal distance $2c$). In the configuration of the SFOC antenna, the far focus of the hyperboloid and the focus of the paraboloid coincide, the angle between their axes equals to $\pi-\beta$, and the feed is located at the near focus of the hyperboloid. For convenience, the coordinate systems of the main reflector and the subreflector are defined. In the coordinate system of the main reflector, the origin is at the parabolic focus, the axis z_m is defined as the axis of the paraboloid, and the axis y_m perpendicularly points out of the paper. In the coordinate system of the subreflector, the origin locates at the center of the two focuses, the axis z_s is chosen as the axis of the hyperboloid, and the axis y_s perpendicularly points out of the paper. Moreover, the projected region of the main reflector is a circle with diameter D on the plane $z_m = 0$, and the offset angle of the main reflector is θ_0 .

Translated from *Journal of Xidian University* (*Natural Science Edition*), 2005, 32(6): 865–869 (in Chinese)

LIU Shao-dong (✉), JIAO Yong-chang, ZHANG Fu-shun
National Laboratory of Antennas and Microwave Technology,
Xidian University, Xi'an 710071, China
E-mail: shdliu@tom.com

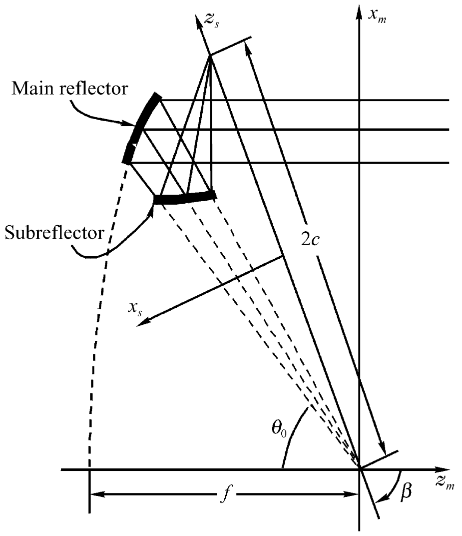

Fig. 1 Geometry of the side-fed offset Cassegrain system

3 Calculation of the average power pattern for SFOC antenna

The root mean square (RMS) error, also called the tolerance, is a standard parameter for measuring the manufacturing precision of the reflector. Ruze [7] presented a useful statistical model for determining the effects of the surface tolerance on the average pattern. During his analysis, the random surface error at any point is defined as the deviation of the error surface from the standard surface in the normal direction, and the error quantity of the point is related to the error status of its neighbor region. The bigger the error quantity of the point is, the larger the error of its neighbor region is. Thus, in the process of analysis, the reflector aperture is partitioned into M small regions with the same size, and the error quantity in each small region is assumed to be identical. Based on this idea, the manufacturing tolerance ε_{RMS} of the reflector is then expressed by:

$$\varepsilon_{\text{RMS}} = \sqrt{\frac{1}{M}\sum_{i=1}^{M}\varepsilon_i^2} \tag{1}$$

where ε_i is the surface error in the ith small area.

Assuming that a ray emanated from the feed intersects with the main reflector at the point P_m (or P'_m) after being reflected at the point P_s (or P'_s) on the subreflector. Figure 2 shows the effect of the random surface errors at the points P_s and P_m in the normal directions on the path length of the ray, where the dot line represents the standard case in which two reflectors have no surface errors, while the solid line denotes the practical case in which the surface errors are introduced. Symbols $\boldsymbol{n}_s$ and $\boldsymbol{n}_m$ are unit vectors in the normal directions at the points P_s and P_m, respectively, while ε_s and ε_m are the corresponding error quantities. In addition, θ_s and θ_m represent the angles of incidence at the points P_s and P_m, respectively. Because both ε_s and ε_m are usually small, the aperture phase error of the ray emanated from the feed and reflected by the main reflector as well as subreflector can be expressed as Ref. [8], namely:

$$\delta = \frac{4\pi}{\lambda}[\varepsilon_s \cos\theta_s + \varepsilon_m \cos\theta_m] \tag{2}$$

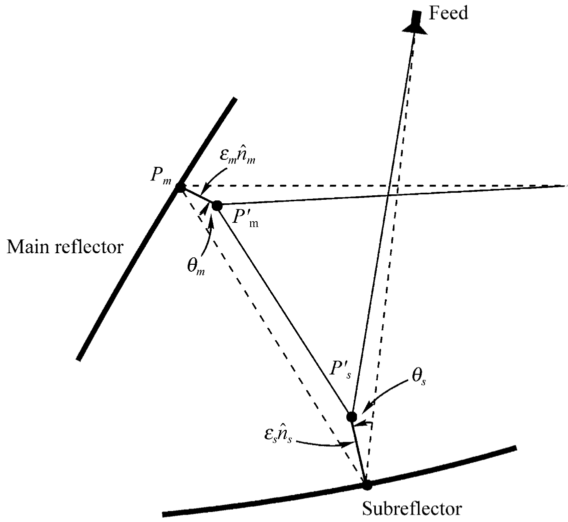

Fig. 2 Effects of random surface errors on the path length of the ray emanated from the feed and arriving at the aperture

According to the aperture integration method, one can obtain the far field of the antenna [9, 10]:

$$E = \iint_A f(\rho',\varphi')\mathrm{e}^{\mathrm{j}\delta}\mathrm{e}^{\mathrm{j}k\boldsymbol{\rho}'\cdot\boldsymbol{r}}\mathrm{d}s' \tag{3}$$

where the function $f(\rho',\varphi')$ is the electric field on the aperture. Assuming that the reflector aperture is partitioned into M small regions with the same size, then Eq. (3) can be rewritten as the following summation:

$$E(\theta,\varphi) = \sum_{i=1}^{M} E_i(\theta,\varphi)\mathrm{e}^{\mathrm{j}\delta_i} \tag{4}$$

where

$$E_i(\theta,\varphi) = f(\rho_i',\varphi_i')\mathrm{e}^{\mathrm{j}k\rho_i'\sin\theta\cos(\varphi-\varphi_i')}\Delta s_i \tag{5}$$

Δs_i is the area of the i th small region. Then, from Eqs. (4) and (5), the power pattern of the antenna is expressed by:

$$EE^* = \sum_{i=1}^{M}\sum_{l=1}^{M} E_i E_l^* \mathrm{e}^{\mathrm{j}(\delta_i-\delta_l)} \tag{6}$$

Assuming that the phase errors δ_i and δ_l are uncorrelated with each other and have a Gaussian amplitude distribution with zero mean and standard deviations σ_i and σ_l, respectively, then the average values of $\mathrm{e}^{\mathrm{j}\delta_i}$ and $\mathrm{e}^{-\mathrm{j}\delta_l}$ can be calculated by:

$$\overline{\mathrm{e}^{\mathrm{j}\delta_i}} = \int_{-\infty}^{\infty}\frac{1}{\sqrt{2\pi\sigma_i^2}}\mathrm{e}^{-\delta_i^2/2\sigma_i^2}\mathrm{e}^{\mathrm{j}\delta_i}\mathrm{d}\delta_i = \mathrm{e}^{-\sigma_i^2/2} \tag{7a}$$

$$\overline{\mathrm{e}^{-\mathrm{j}\delta_l}} = \int_{-\infty}^{\infty} \frac{1}{\sqrt{2\pi\sigma_l^2}} \mathrm{e}^{-\delta_l^2/2\sigma_l^2} \mathrm{e}^{-\mathrm{j}\delta_l} \mathrm{d}\delta_l = \mathrm{e}^{-\sigma_l^2/2} \tag{7b}$$

According to Eq. (2), the standard deviation σ_i in Eq. (7a) (σ_l in Eq. (7b) is similar) can be obtained by:

$$\sigma_i = \frac{4\pi}{\lambda}\left[(\varepsilon_s)_{\mathrm{rms}}^i \cos\theta_s + (\varepsilon_m)_{\mathrm{rms}}^i \cos\theta_m \right] \tag{8}$$

where $(\varepsilon_s)_{\mathrm{RMS}}^i$ and $(\varepsilon_m)_{\mathrm{RMS}}^i$ are the RMS surface errors corresponding to the ith small regions on the aperture of the main and subreflector, respectively. From Eqs. (7a) and (7b), we can obtain the average value of the function $\mathrm{e}^{\mathrm{j}(\delta_i-\delta_l)}$

$$\overline{\mathrm{e}^{\mathrm{j}(\delta_i-\delta_l)}} = \begin{cases} \mathrm{e}^{-\left(\sigma_i^2+\sigma_l^2\right)/2}, & \delta_i \neq \delta_l \\ 1, & \delta_i = \delta_l \end{cases} \tag{9}$$

Equation (2) is used to judge whether δ_i is equal to δ_l or not.

Finally, from Eqs. (6) and (9), the average power pattern of the SFOC antenna can be expressed by

$$\overline{EE^*} = \sum_{i=1}^{M}\sum_{l=1}^{M} E_i E_l^* \mathrm{e}^{-\left(\sigma_i^2+\sigma_l^2\right)/2} + \sum_{\substack{i=1 \\ \delta_i=\delta_l}}^{M}\sum_{l=1}^{M} E_i E_l^* \left(1-\mathrm{e}^{-\sigma_i^2}\right) \tag{10}$$

and the variance of the power pattern can be obtained from Eqs. (6) and (10),

$$D(EE^*) = \frac{1}{N}\sum_{i=1}^{N}\left[\left(EE^*\right)_i - \left(\overline{EE^*}\right)_i \right]^2 \tag{11}$$

where $\left(EE^*\right)_i$ and $\left(\overline{EE^*}\right)_i$ represent the values of the power pattern and the average power pattern in the ith sample direction, respectively, and N is the number of total sample directions.

4 Numerical results

In this section, a general computer program has been written for analyzing the average power pattern of the SFOC antenna whose main parameters (refer to Fig. 1) are given in Table 1. Like the simulation results, the related data and curves are also presented in the following, which demonstrate the effects of surface random errors on the antenna's gain and side lobe levels. We hope that these results would be helpful for the designers to determine the manufacturing accuracy of the reflector. In our analysis, the feed is x-polarized, and its E- and H-plane patterns are approximated by $\cos^{72}\theta$ (In the case, the level in the edge of the subreflector is –15 dB).

Table 1 Main parameters of the SFOC antenna

Aperture (D)	100 λ
Offset angle of the main reflector (θ_0)	58.3°
Focal length of the main reflector (f)	429.08 λ
Half focal length of the subreflector (c)	295.98 λ
Eccentricity of the subreflector (e)	2.239 3
Angle β	70.0°

Figure 3 shows the average power pattern of the SFOC antenna with the standard main reflector (paraboloid) and various subreflector surface errors. In Fig. 3, every value is normalized to the directivity of the antenna in the case where the main reflector and the subreflectors are absent of surface errors. In order to reveal clearly the effects of the random surface errors on the gain and the side lobe levels, Fig. 4 presents the corresponding peak gain loss and side lobe level increase versus the subreflector surface errors. In Fig. 4, the peak gain loss is the difference between the gains of the actual antenna and the standard antenna (free of surface error), and the side lobe increase is the difference between the side lobe levels of them. Similarly, Fig. 5 shows the average power pattern of the SFOC antenna with the standard subreflector (hyperboloid) and various main reflector surface errors. Figure 6 presents the corresponding peak gain loss and side lobe level increase versus the main reflector surface errors.

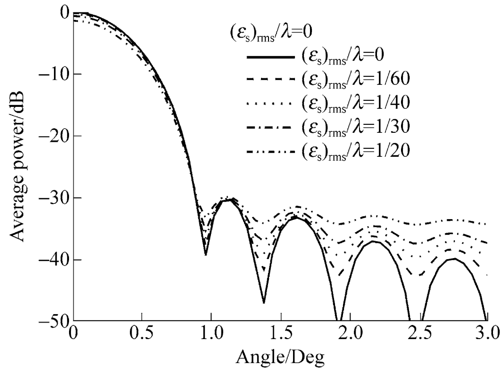

Fig. 3 Average power pattern of the SFOC antenna with the standard main reflector (paraboloid) and various subreflector surface errors

From Fig. 3–6, one can see that the random surface errors result in the peak gain loss and the side lobe level increase, and the effect is evident for the second and third side lobe levels. Furthermore, from the relation of the tolerance value with the side lobe level, we can clearly see that as the side lobe level decreases, the manufacturing accuracy of the reflector increases, and its dependence on the surface error becomes much stronger. For a specified tolerance level, a considerably smaller surface error is required to maintain the low side lobe levels within the required bounds. In addition, we draw a conclusion from Fig. 3–6 that the effect of the subreflector surface error on the antenna performance is a little stronger than the main reflector surface error, which is comprehensible from the configuration of the SFOC antenna. As the feed of the SFOC antenna is mounted above the main reflector, the angle of incidence of a specified ray for the subreflector is smaller than that for the main reflector. Thus, according to Eq. (2), the subreflector surface error has a greater effect on the total path length of the ray than the main surface error. However, for the main reflector and subreflector surface errors, the difference of their effects on the peak gain loss and the side lobe level increase is not evident.

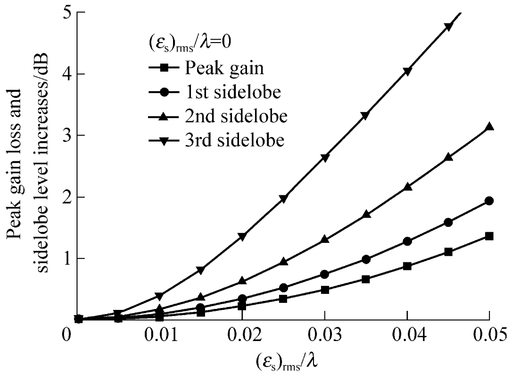

Fig. 4 Peak gain loss and sidelobe level increase versus the subreflector surface error for the SFOC antenna with the standard main reflector (paraboloid)

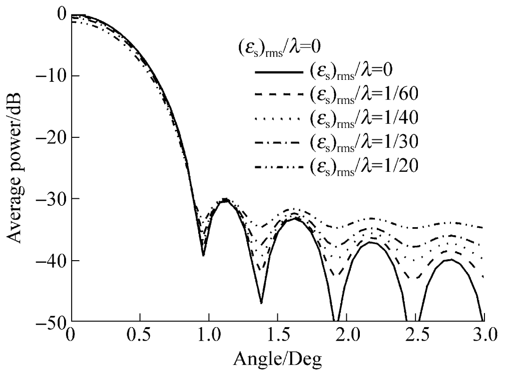

Fig. 5 Average power pattern of the SFOC antenna with the standard subreflector (hyperboloid) and various main reflector surface errors

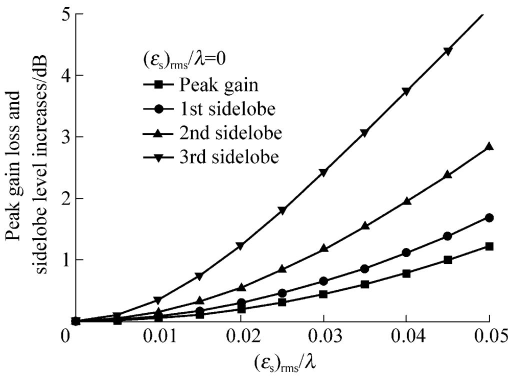

Fig. 6 Gain loss and sidelobe level increase versus the main reflector surface errors for the SFOC antenna with the standard subreflector (hyperboloid)

Taking the main reflector surface error as $\lambda/40$, Fig. 7 shows the peak gain loss and the side lobe level increase versus the subreflector surface error. Figure 8 presents the peak gain loss versus the subreflector surface error when the main reflector surface error is chosen as some given values. These curves can be readily employed by the user to determine an appropriate accuracy requirement according to the realistic situation on the SFOC antenna's reflector.

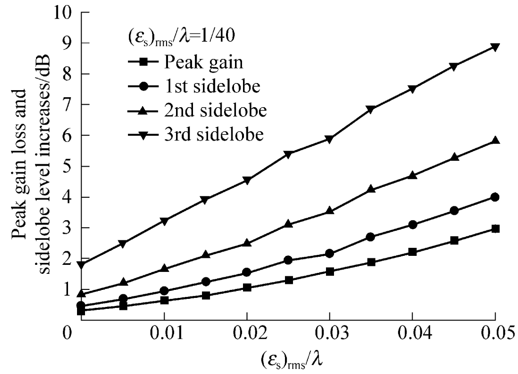

Fig. 7 Peak gain loss and sidelobe level increase versus the subreflector surface error for the SFOC antenna when the main reflector surface error is set to $\lambda/40$

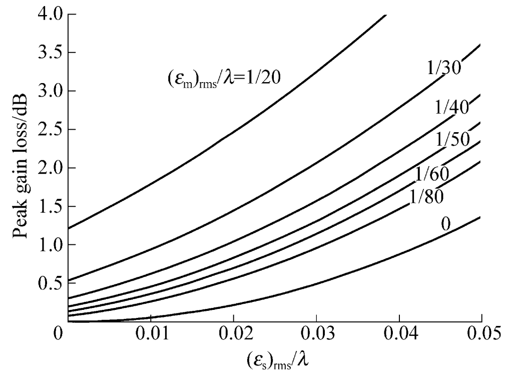

Fig. 8 Peak gain loss versus the subreflector surface error when the main reflector surface error is chosen as some given values

5 Conclusions

Among various errors which affect the reflector antenna's radiation performance, the reflector random surface error is an error source that should be considered in the production of the reflector antennas. In this paper, the average power pattern of the SFOC antenna is analyzed by the numerical method, and the effects of the main reflector and subreflector surface errors on the peak gain loss and the side lobe level increase are introduced. Some simulation data and curves are also given, which will be helpful for determining the reasonable tolerance requirements for manufacturing the reflector antennas.

Acknowledgements This work was supported by the National Natural Science Foundation of China (No. 60171045), the Excellent Young Teachers Program, Ministry of Education, China.

References

1. Lei Juan, Wan Ji-xiang, Fu De-min et al., Design and analysis of a multi-beam parabolic reflector antenna, Journal of Xidian University, 2003, 30 (3): 399–402 (in Chinese)
2. Olver A. D., Tolerances on millimetre wave reflector antennas, IEE Colloquium on Reflector Antennas for the 90's, 1992: 1–4
3. Pontoppidan K., Reflector surface tolerance effects, IEEE Antennas and Propagation Society International Symposium, 1986, 24: 413–416
4. Lindley A., Analysis of distorted reflector antennas, Sixth International Conference on Antennas and Propagation (Conf. Publ. No.301), 1989, 1: 32–34
5. Hao Ling, Yuen Lo, Rahmat-Sami Y., Reflector sidelobe degradation due to random surface errors, IEEE Transactions on Antennas and Propagation, 1986, 34 (2): 164–172
6. Jorgensen R., Balling P., Dual offset reflector multibeam antenna for international communications satellite applications, IEEE Transactions on Antennas and Propagation, 1985, 33 (12): 1304–1312
7. Ruze J., Antenna tolerance theory-A review, Proc. IEEE, 1966, 54 (4): 633–640
8. Rusch W., Wohlleben R., Surface tolerance loss for dual-reflector antennas, IEEE Transactions on Antennas and Propagation, 1982, 30 (4): 784–785
9. Kim J. W, Kim B. S, Computation of the average power pattern of a reflector antenna with random surface errors and misalignment errors, IEEE Transactions on Antennas and Propagation, 1996, 44 (7): 996–999
10. Rahmat-Samii Y., An efficient computational method for characterizing the effects of random surface errors on the average power pattern of reflectors, IEEE Transactions on Antennas and Propagation, 1983, 31 (1): 92–98